Eur. J. Mineral., 36, 311–322, 2024
https://doi.org/10.5194/ejm-36-311-2024

European Journal of Mineralogy
Open Access

Igelströmite, $Fe^{3+}(Sb^{3+}Pb^{2+})O_4$, and manganoschafarzikite, $Mn^{2+}Sb_2^{3+}O_4$, two new members of the newly established minium group, from the Långban Mn–Fe deposit, Värmland, Sweden

Dan Holtstam[1], Jörgen Langhof[1], Henrik Friis[2], Andreas Karlsson[1], and Muriel Erambert[3]

[1]Department of Geosciences, Swedish Museum of Natural History, P.O. Box 50007, 104 05 Stockholm, Sweden
[2]Natural History Museum, University of Oslo, P.O. Box 1172, Blindern, 0318 Oslo, Norway
[3]Department of Geosciences, University of Oslo, P.O. Box 1047, Blindern, 0316 Oslo, Norway

Correspondence: Dan Holtstam (dan.holtstam@nrm.se)

Received: 28 December 2023 – Revised: 8 February 2024 – Accepted: 10 February 2024 – Published: 25 March 2024

Abstract. The two new minerals igelströmite, $Fe^{3+}(Sb^{3+}Pb^{2+})O_4$, and manganoschafarzikite, $Mn^{2+}Sb_2^{3+}O_4$, are found in the Långban Fe–Mn deposit, in open fractures in a fine-grained hematite ore, with minor amounts of aegirine, a serpentine-group mineral, fluorcalcioroméite, baryte, nadorite, mimetite and other late-stage minerals. Igelströmite is named after the Swedish geologist–mineralogist Lars Johan Igelström (1822–1897).

Mohs hardness = 3–4 and $D_{calc} = 6.33(1)$ and $5.37(2)\,g\,cm^{-3}$ for igelströmite and manganoschafarzikite, respectively. Cleavage is distinct on {110}. Both minerals are brittle, with an uneven to conchoidal fracture. The chemical formulae obtained from microprobe data are $(Fe^{3+}_{0.59}Mn^{2+}_{0.29}As^{3+}_{0.06}Fe^{2+}_{0.06})_{\Sigma=1.00}(Sb^{3+}_{1.24}Pb^{2+}_{0.65}As^{3+}_{0.11})_{\Sigma=2.00}O_4$ and $(Mn^{2+}_{0.64}Fe^{2+}_{0.25}Mg_{0.08})_{\Sigma=0.97}(Sb^{3+}_{1.97}As^{3+}_{0.03}Pb^{2+}_{0.01})_{\Sigma=2.01}O_4$. The crystal structures for igelströmite and manganoschafarzikite have been refined in space group $P4_2/mbc$ from single-crystal X-ray diffraction data to $R1 = 3.73\,\%$ and $1.51\,\%$, respectively, giving the following sets of unit-cell parameters: $a = 8.4856(2)$, $8.65159(8)$ Å; $c = 6.0450(3)$, $5.97175(9)$; and $V = 435.27(3)$, $446.986(11)$ Å^3 for $Z = 4$. Both minerals are isostructural with minium, $Pb^{4+}Pb_2^{2+}O_4$, where $Pb^{4+}O_6$ forms distorted octahedra, which connect via trans-edges to form rutile-like ribbons along c. The Pb^{2+} atoms appear in trigonal, flattened PbO_3 pyramids, which are linked via corners to form zigzag $(PbO_2)_n$ chains. The minium group, of general formula MX_2O_4 ($X = As^{3+}$, Sb^{3+}, Pb^{2+}), presently consists of the minerals minium, trippkeite, schafarzikite, igelströmite and manganoschafarzikite. For future new members, it is recommended to consider the X cation content for the root name and add prefixes to indicate the dominant metal at the M position.

1 Introduction

In the course of examining undescribed fissure minerals from the Långban Mn–Fe deposit, in the geological collections of the Swedish Museum of Natural History, two new and closely related minerals have been discovered: igelströmite ($Fe^{3+}(Sb^{3+}Pb^{2+})O_4$; IMA2021-035; mineral symbol: Ig) and manganoschafarzikite ($Mn^{2+}Sb_2^{3+}O_4$; IMA2022-129; Msfz).

Igelströmite and manganoschafarzikite are isostructural with known minerals of the general formula MX_2O_4, including trippkeite, schafarzikite and minium (Table 1). Minium, ideally $Pb^{4+}Pb_2^{2+}O_4$, is the oldest named of these species. The word "minium" (derived from the river Minius, now called Minho, in Iberia) is ancient, used by e.g. Pliny the

Elder (*Naturalis Historia*, book XXXIII, Chap. LX; Rackham, 1952), who mentioned two kinds; one is corresponding to cinnabar, and the other one is a reddish substance obtained from heat treatment of silver–lead ores. By the end of the Renaissance, "minium" was used solely for the compound Pb_3O_4 (red lead pigment; the *minium secundarium* of Agricola, 1912). Methods of producing minium artificially were also known in China during the Han dynasty, 202 BCE–220 CE (Gettens et al., 1972).

Smithson (1806) provided a confirmation of minium existing as a natural mineral in a sample of galena from Germany. Minium thus has priority over trippkeite, described by Damour and vom Rath (1880) from Copiapó Province, Chile, as a group name. Schafarzikite was first reported by Krenner (1921) from Krížnica hill, Slovakia. The Commission on New Minerals, Nomenclature and Classification (CNMNC) of the International Mineralogical Association (IMA) has approved the minium group (proposal 23-C) and the two new minerals described herein.

Igelströmite is named after Lars Johan Igelström (1822–1897), who demonstrated the existence of manganese ores at Långban and the nearby mineral localities Harstigen, Pajsberg, Nordmark, Jakobsberg and Sjögruvan. Among other things, he was also the first geologist to note the peculiar occurrence of native lead at Långban in 1871 (Langhof, 1999). The mineral name igelströmite has been used twice previously: first, as a synonym never given species status (and misspelled "ingelstromite"), for a colour variety of pyroaurite (Heddle, 1878), a mineral originally described by Igelström (1865) from Långban, and the second time by Weibull (1883) for an intermediate member of the tephroite–fayalite series with composition range 20 %–40 % Mn_2SiO_4, and thus it was never accepted as a separate species. The holotype material (specimen and epoxy mount) is deposited in the type mineral collection of the Department of Geosciences, Swedish Museum of Natural History, P.O. Box 50007, 10405 Stockholm, Sweden, under collection number GEO-NRM 19255056. This specimen was originally designated as a duplicate of no. 66 on a list of Långban unknowns (Flink, 1921). The true no. 66 has, however, been identified as valentinite and is not from the same mineral association as igelströmite. Material taken from the sample for the crystallographic investigation is stored at the Natural History Museum in Oslo (KNR 44278).

Manganoschafarzikite is named as the Mn analogue of schafarzikite. Holotype material is GEO-NRM 19339699, of which a fragment, used for structure determination and chemical analyses, is kept in Oslo (KNR 44410).

2 Occurrence

At the Långban deposit (Filipstad, Värmland, Sweden; 59.85° N, 14.26° E; 215 m a.s.l.) distinct hausmannite–braunite and magnetite–hematite ore bodies are hosted by Palaeoproterozoic (∼ 1.9 Ga) dolomitic marbles. The presence of deformed ore masses, recrystallized skarn assemblages, and several generations of cavity and fissure minerals testifies to a complex geological evolution, under variable temperature and pressure conditions (Holtstam and Langhof, 1999). The Långban mine is a source of many rare minerals, and the number of type species exceeds 75, likely making it the most prolific mineral deposit in the solar system (https://www.mindat.org/loc-3167.html, last access: 27 December 2023). The Långban-type Fe–Mn–(Ba–Pb–As–Sb–Be) deposits found scattered in the SW part of the Bergslagen ore region are originally derived by precipitation from metal-enriched volcanogenic solutions on a shallow ocean carbonate floor, and subsequently subject to metamorphism and metasomatic alteration (Boström et al., 1979; Holtstam and Mansfeld, 2001).

The two new minerals occur on open fractures in a fine-grained, bluish-grey hematite ore, with minor amounts of aegirine, a serpentine-group mineral and fluorcalcioroméite. The fractures are subparallel to each other, and some are filled with grey to white calcite. The most conspicuous mineral in these fractures is bright-yellow nadorite, as euhedral tablet-formed single crystals or intergrown aggregates. Igelströmite (Fig. 1) is associated with thin tabular hematite, colourless baryte, senarmontite, white acicular mimetite up to 1 mm and grey globular aggregates of Pb-bearing rhodochrosite. The substrate for the above-mentioned minerals, including igelströmite, is a greyish-black serpentine-group mineral as globular masses. The crystallization sequence established from the few known specimens is hematite → baryte → "serpentine-group mineral" → igelströmite → nadorite → senarmontite → mimetite → rhodochrosite. So far only four specimens containing igelströmite have been encountered in the mineral collection of the Swedish Museum of Natural History, which houses approximately 25 000 Långban specimens, and hence the mineral must be regarded as very rare.

Manganoschafarzikite (Fig. 2) was discovered during a search for additional samples of igelströmite. So far, only the type specimen exists. Associated minerals are thin tabular hematite, andradite, calcite, rounded aggregates of native lead with a white thin coating of hydrocerussite, small grey-white globular aggregates of lead-bearing rhodochrosite and rarely white acicular mimetite. The substrate is the same serpentine-group mineral as noted for igelströmite. The inferred crystallization sequence here is hematite → andradite → baryte → serpentine-group mineral → lead → nadorite → manganoschafarzikite → mimetite → rhodochrosite.

With a good probability, the specimens of the two new minerals originate from the *Hindenburg* working in the mine, where most of the nadorite specimens of the present type were encountered (Flink, 1923). The label assigned to the igelströmite type sample states the *Japan* drift, but this might be an error, a mere confusion through the association with

Table 1. Members of the minium group.

	Minium	Trippkeite	Schafarzikite	Igelströmite	Manganoschafarzikite
Ideal formula	$Pb^{4+}Pb_2^{2+}O_4$	$Cu^{2+}As_2^{3+}O_4$	$Fe^{2+}Sb_2^{3+}O_4$	$Fe^{3+}(Sb^{3+}Pb^{2+})O_4$	$Mn^{2+}Sb_2^{3+}O_4$
Type locality		Copiapó, Chile	Krížnica, Slovakia	Långban, Sweden	Långban, Sweden
Space group	$P4_2/mbc$	$P4_2/mbc$	$P4_2/mbc$	$P4_2/mbc$	$P4_2/mbc$
Unit-cell parameters	$a = 8.811$ Å $c = 6.563$ Å $Z = 4$ $V = 509.51$ Å^3	$a = 8.592$ Å $c = 5.573$ Å $Z = 4$ $V = 411.41$ Å^3	$a = 8.6073(2)$ Å $c = 5.9093(3)$ Å $Z = 4$ $V = 437.80(2)$ Å^3	$a = 8.4856(2)$ Å $c = 6.0450(3)$ Å $Z = 4$ $V = 435.27(3)$ Å^3	$a = 8.65159(8)$ Å $c = 5.97175(9)$ Å $Z = 4$ $V = 446.986(11)$ Å^3
Reference	Gavarri and Weigel (1975)	Zemann (1951b)	Sejkora et al. (2007)	This work	This work

Figure 1. The type specimen of igelströmite showing a black aggregate of lenticular, parallel-grown igelströmite crystals on blackish globular "serpentine", with associated yellow nadorite and greyish-colourless aggregates of lead-bearing rhodochrosite. Field of view is ca. 4 × 3 mm. GEO-NRM 19255056. Photo: Torbjörn Lorin.

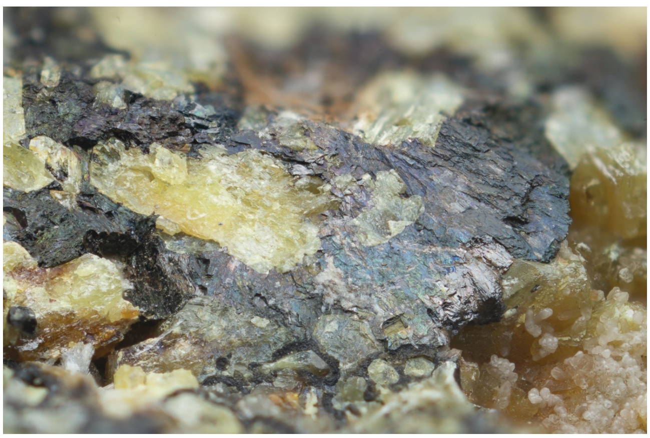

Figure 2. The type specimen of manganoschafarzikite showing a tarnished dark-red-brown to black lamellar aggregate of manganoschafarzikite surrounding yellow nadorite. At the bottom-right corner, greyish to white crystals of rhodochrosite appear. Image width 6 mm. GEO-NRM 19339699. Photo: Torbjörn Lorin.

Flink's no. 66. *Hindenburg* was mined for Fe and Mn ore at the 150 m level, from 1916 to 1928 and was finally worked through into the *England* stope at the 165 m level (Magnusson, 1930).

3 Physical and optical properties

Igelströmite occurs as lenticular crystals forming compact crystal aggregates of rounded appearance, up to 1 mm across (Fig. 1). Manganoschafarzikite forms platy aggregates up to 5 mm, with a conspicuous peacock tarnish on crystal surfaces (Fig. 2). Both minerals are dark reddish-brown to black in colour, with translucent thin edges and a submetallic lustre. The streak is yellowish brown to dark brown. Hardness could not be measured on the small crystals available; the estimated Mohs hardness is 3–4, in analogy with schafarzikite. Cleavage is distinct/good on {110}. Both minerals are brittle, with an uneven to conchoidal fracture. The calculated densities, based on empirical chemical formulae and the unit cell from single-crystal data, are 6.33(1) and 5.37(2) g cm^{-3} for igelströmite and manganoschafarzikite, respectively.

Both minerals are greyish-white in plane-polarized light under the microscope in polished sections and weakly bireflectant and nonpleochroic. Internal reflections in dark brown to red are present. Reflectance spectra were collected with an AvaSpec-ULS2048 × 16 spectrometer connected to a Zeiss Axiotron UV microscope (10× and 0.20 Ultrafluar objective), using a W filament lamp and a dichroic polaroid filter. SiC (Zeiss no. 846) was used as standard, and the circular area of measurement was about 0.1 mm in diameter. Results from the 400–70 nm range are given in Table 2. Overall, igelströmite is slightly more reflectant (about 1 % absolute) than manganoschafarzikite.

4 Chemical composition

Crystal fragments of the minerals were mounted in epoxy resin, polished and carbon-coated prior to analysis. Electron probe microanalysis (EPMA) was performed with a Cameca SX100 instrument (at the Department of Geosciences,

Table 2. Reflectance values (%) measured in air, with Commission on Ore Mineralogy (COM) wavelengths in bold, for igelströmite (Ig) and manganoschafarzikite (Msfz).

	Ig		Msfz			Ig		Msfz	
λ (nm)	R_2	R_1	R_2	R_1	λ	R_2	R_1	R_2	R_1
400	16.8	15.9	16.4	15.2	560	15.0	14.3	14.6	13.7
420	16.7	15.8	16.0	14.8	580	14.9	14.3	14.4	13.4
440	16.6	15.6	15.7	14.5	**589**	**14.9**	**14.2**	**14.4**	**13.4**
460	16.2	15.4	15.5	14.2	600	14.8	14.2	14.3	13.3
470	**16.1**	**15.2**	**15.4**	**14.1**	620	14.7	14.1	14.2	13.3
480	15.9	15.1	15.2	14.0	640	14.9	14.2	14.1	13.2
500	15.6	14.8	15.0	13.8	**650**	**14.8**	**14.1**	**14.1**	**13.2**
520	15.3	14.6	14.8	13.7	660	14.7	14.0	14.1	13.2
540	15.2	14.4	14.7	13.6	680	14.7	14.1	14.0	13.1
546	**15.1**	**14.4**	**14.7**	**13.6**	700	14.5	13.8	14.0	13.1

University of Oslo) running at 15 kV, with sample current 10 nA (manganoschafarzikite) or 15 nA (igelströmite) and beam diameter in the range of 2–10 µm. Bi and Zn (also Mg for igelströmite) were analysed for but not detected. The analytical data are collected in Table 3, along with the reference materials used in the measurements. The low totals for igelströmite are probably related to incomplete conduction on a small fragment surface embedded in epoxy. The empirical formula for igelströmite, recalculated on the basis of three cations and with Fe^{3+} / Fe^{2+} recast to achieve overall charge balance, is $(Fe^{3+}_{0.59}Mn^{2+}_{0.29}As^{3+}_{0.06}Fe^{2+}_{0.06})_{\Sigma=1.00}$-$(Sb^{3+}_{1.24}Pb^{2+}_{0.65}As^{3+}_{0.11})_{\Sigma=2.00}O_4$. The empirical formula of manganoschafarzikite, on a four-anion basis, is $(Mn^{2+}_{0.64}Fe^{2+}_{0.25}Mg_{0.08})_{\Sigma=0.97}(Sb^{3+}_{1.97}As^{3+}_{0.03}Pb_{0.01})_{\Sigma=2.01}O_4$.

The ideal formula of igelströmite is $Fe(SbPb)_{\Sigma=2}O_4$, which requires Fe_2O_3 17.79, Sb_2O_3 32.48 and PbO 49.73, total 100 wt %. The corresponding formula for manganoschafarzikite is $MnSb_2O_4$ and requires MnO 19.57 and Sb_2O_3 80.43, total 100 wt %. There is no indication of H_2O, CO_2 or other volatiles being present in these minerals, from structural or spectroscopic data.

5 X-ray diffraction data and structure refinement

5.1 Crystal structure refinement

Intensity X-ray diffraction data for single-crystal structure analysis were collected at room temperature with monochromated Mo$K\alpha$ radiation (λ = 0.71703 Å, obtained at 50 kV and 1 mA) on a Rigaku Synergy-S diffractometer equipped with a HyPix-6000HE detector hosted at the Natural History Museum (NHM) in Oslo. The instrument has kappa geometry, and both data collection and subsequent data reduction and face-based absorption corrections were carried out using the CrysAlis^{Pro} software. See Table 4 for details of data collection and refinement. The crystal structures were solved by direct methods and refined using neutral atom scattering factors with SHELXL (Sheldrick, 2015). The WinGX interface was used for the refinement (Farrugia, 2012). The crystal structures for igelströmite and manganoschafarzikite were refined to $R1$ 3.73 % and 1.51 %, respectively. Crystallographic information files (CIFs) are available in the Supplement to this paper.

Because of the high amount of Pb at the site dominated by Sb^{3+}, the structure of igelströmite was refined with lower symmetries to explore potential ordering and splitting of the Sb site. None of these refinements provided a better result, and when checking the resulting CIF files, the *CheckCIF* routine always suggested the chosen tetragonal symmetry. In the final stages of refinement, the Sb site was refined as a mixed Sb–Pb site. Tables 5 and 6 present the atomic coordinates and site occupancies, respectively. Table 7 contains anisotropic thermal parameters and bond distances.

For manganoschafarzikite, after all atoms had been refined anisotropically, the occupancy for the two cation sites was released. As the Sb site refined to 1, it was constrained to this value in the final refinements. The occupancy of the Mn site was slightly below 1 due to the presence of Mg at that site. In the final refinement, the proposed weighting scheme was applied (Table 4). Tables 8 and 9 contain the fractional coordinates and atom displacement factors for manganoschafarzikite. Table 10 shows the calculated bond distances for both minerals.

5.2 Powder data

X-ray powder diffraction data were collected on single-crystal fragments using the same diffractometer as above utilizing the Gandolfi movement and Cu$K\alpha$ radiation (λ = 1.54184 Å at 50 kV and 1 mA). The unit-cell parameters were refined using the program UnitCell (Holland and Redfern, 1997). The unit-cell parameters refined from the powder data for igelströmite based on 18 reflections are a = 8.4777(5) Å, c = 6.0417(6) Å and V = 434.23(5) Å^3, and for manganoschafarzikite based on 23 reflections, they

Table 3. Chemical data (in wt %) for igelströmite and manganoschafarzikite. n denotes number of point analyses.

Constituent	Igelströmite		Manganoschafarzikite		Reference material
	Mean, $n = 12$	2σ	Mean, $n = 7$	2σ	
MgO	–	–	0.89	0.10	Synthetic MgO
MnO	4.78	1.57	12.72	0.42	Pyrophanite
FeO	1.14	1.92	4.98	0.23	Pure metal
Fe_2O_3	11.05	1.73			Pure metal
As_2O_3	3.88	1.41	0.96	0.10	Synthetic AsGa
Sb_2O_3	42.89	5.41	80.15	0.38	Synthetic Sb_2S_3
PbO	34.42	4.53	0.92	0.24	Vanadinite
Total	98.17		100.62		

Table 4. Single-crystal data collection and refinement parameters for igelströmite and manganoschafarzikite. GoF denotes goodness of fit.

	Igelströmite	Manganoschafarzikite
Crystal size (mm)	0.007 × 0.028 × 0.041	0.040 × 0.060 × 0.110
Space group	$P4_2/mbc$ (no. 135)	$P4_2/mbc$ (no. 135)
a (Å)	8.4856(2)	8.65159(8)
c (Å)	6.0450(3)	5.97175(9)
V (Å^3)	435.27(3)	446.986(11)
Z	4	4
$D_{calc.}$ (g cm^{-3})	6.33(1)	5.37(2)
Number of reflections	6571	31859
Unique reflections	500	475
Reflections $Fo > 4\sigma$ (Fo)	411	462
Diffraction limits	$-12 \leq h \leq 13$;	$-13 \leq h \leq 13$;
	$-13 \leq k \leq 13$;	$-12 \leq k \leq 13$;
	$-9 \leq l \leq 9$	$-9 \leq l \leq 9$
Max 2θ (°)	70.22	67.21
R_{int} (%)	3.93	3.87
R_σ (%)	1.81	0.007
$R1$ for $Fo > 4\sigma$ (Fo) (%)	3.73	1.51
$R1$ for all (%)	4.60	1.57
$wR2$ (%)	6.66	3.74
GoF	1.315	1.233
$\Delta\rho_{max}$ (e Å^{-3})	1.22 at 1.57 Å from O2	0.89 at 0.77 Å from Sb
$\Delta\rho_{min}$ (e Å^{-3})	−1.62 at 0.68 Å from Sb	−0.79 at 0.53 Å from Sb

Note: weight Ig $= 1 / [\sigma^2(Fo^2) + (0.00 \times P)^2 + 7.38 \times P]$, where $P = (\max(Fo^2, 0) + 2 \times Fc^2)/3$. Weight Msfz $= 1 / [\sigma^2(Fo^2) + (0.0127 \times P)^2 + 1.2324 \times P]$, where $P = (\max(Fo^2, 0) + 2 \times Fc^2)/3$.

are $a = 8.6273(5)$ Å, $c = 5.9683(5)$ Å and $V = 442.23(5)$ Å^3. The complete sets of X-ray powder diffraction data are shown in Table 11.

6 Spectroscopy

6.1 Micro-Raman spectroscopy

Laser micro-Raman measurements were carried out using a Horiba (Jobin Yvon) LabRAM HR Evolution on randomly oriented crystals. The samples were excited with a frequency-doubled 532 nm Nd:YAG laser utilizing an Olympus 100× objective (numerical aperture (NA) = 0.9). Raman spectra of the samples were collected through two acquisition cycles with single counting times of 90 s. Spectra were generated in the range of 200 to 4000 cm^{-1} with a 1800 grooves cm^{-1} grating and a thermoelectrically cooled electron multiplier charge-coupled device (CCD). The wavenumber calibration was performed using the 520.7 cm^{-1} Raman band on a silicon standard, with a wavenumber accuracy of around 1 cm^{-1}. For igelströmite, no usable spectrum could be obtained due to laser-induced breakdown of the sample surface. In manganoschafarzikite (Fig. 3), bands are observed at 669, 543, 522, 460, 402, 348,

Table 5. Fractional coordinates and bond-valence sums (BVS) for igelströmite. SOF denotes site occupancy factor.

Site	x	y	x	U^{iso}	SOF	BVS*
Sb	0.65890(7)	0.33689(6)	0	0.0235(2)	0.76(3)	2.40
Pb	0.65890(7)	0.33689(6)	0	0.0235(2)	0.24(3)	–
Fe	1/2	0	1/4	0.0122(4)	0.978(17)	2.60
O1	0.8253(5)	0.3253(5)	3/4	0.0272(18)	1	1.99
O2	0.6348(8)	0.0964(9)	0	0.0241(17)	1	1.71

* BVS calculated based on mixed-site occupancy (Table 6) and values from Gagné and Hawthorne (2015).

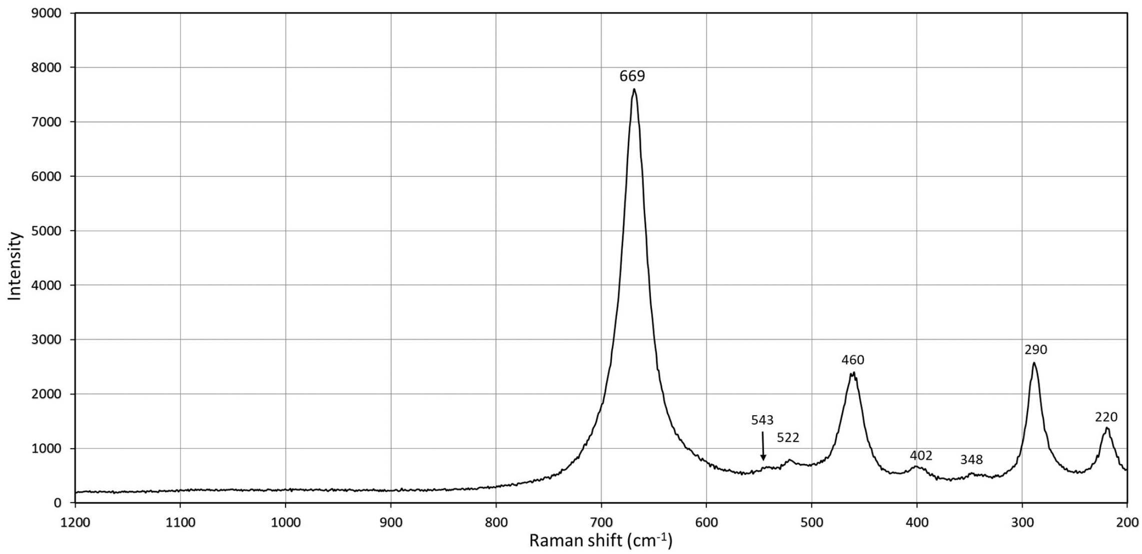

Figure 3. Raman spectrum of manganoschafarzikite.

Table 6. Site-scattering values and composition of igelströmite. SXRD denotes single-crystal X-ray diffraction.

Site	SXRD (e)	Site composition	EPMA (e)
Sb	58.44	$Sb_{0.625}Pb_{0.325}As_{0.055}$	60.34
Fe	25.22	$Fe^{3+}_{0.59}Mn^{2+}_{0.29}Fe^{2+}_{0.06}As_{0.06}$	26.13

290 and 220 cm^{-1}; no spectral features were observed at higher wavenumbers. The strongest peak at 669 cm^{-1} is ascribed to Sb–O symmetric stretching and the weak one at 522 to antisymmetric stretching. The strong band at 460 cm^{-1} may be related to Mn–O stretching or to Sb–O–Sb bending. Other bands at 405 cm^{-1} (weak), 348 (very weak), 290 cm^{-1} (strong) and 220 cm^{-1} (medium) are attributed to Sb–O–Sb bending. The only band that unequivocally can be attributed to Mn–O stretching is the very weak band at 543 cm^{-1}. Overall, the spectrum is quite similar to spectra obtained on schafarzikite (Sejkora et al., 2007; Kharbish, 2012).

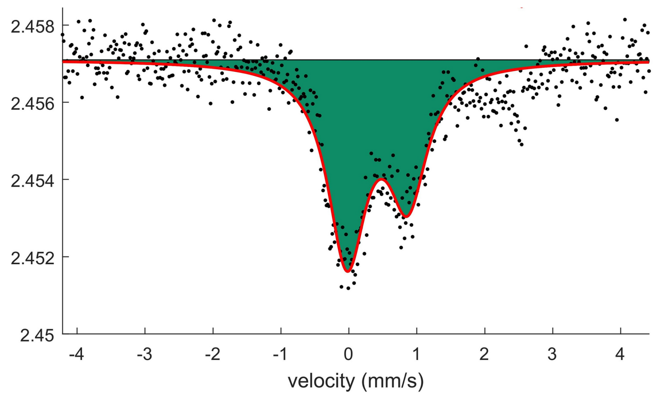

Figure 4. Fitted ^{57}Fe Mössbauer spectrum of igelströmite crystals obtained with a point source.

6.2 Mössbauer spectroscopy

Mössbauer spectroscopy was done employing a conventional spectrometer system operated in constant-acceleration mode. Due to limited amounts of igelströmite, a ^{57}Co rhodium-matrix point source (nominal activity 0.37 GBq) was used.

Table 7. Atomic displacement factors (Å^2) for igelströmite.

Site	U^{11}	U^{22}	U^{33}	U^{23}	U^{13}	U^{12}
Sb	0.0339(4)	0.0209(3)	0.0155(2)	0	0	−0.00842(19)
Pb	0.0339(4)	0.0209(3)	0.0155(2)	0	0	−0.00842(19)
Fe	0.0135(5)	0.0135(5)	0.0098(6)	0	0	0.0011(6)
O1	0.030(2)	0.030(2)	0.022(3)	−0.006(2)	0.006(2)	−0.017(3)
O2	0.022(3)	0.033(4)	0.018(3)	0	0	−0.004(3)

Table 8. Sites, fractional atom coordinates, site occupancies (s.o.), equivalent isotropic displacement parameters (Å^2) and bond-valence sums (BVS) for manganoschafarzikite.

Site	x	y	z	U_{eq}	s.o.	BVS*
Sb	0.17790(2)	0.16695(2)	0	0.01295(7)	$Sb_{1.00}$	2.72
Mn	1/2	0	1/4	0.01167(19)	$Mn_{0.969(4)}$	2.28
O1	0.17947(18)	0.32053(18)	1/4	0.0186(5)	$O_{1.00}$	2.05
O2	0.3999(3)	0.1427(3)	0	0.0151(4)	$O_{1.00}$	1.80

* BVS calculated based on mixed-site occupancy from the empirical formula and values from Gagné and Hawthorne (2015).

Three small (200–250 µm across) randomly oriented grains were attached on plastic tape and positioned close to the source. A spectrum (Fig. 4) was collected over 1024 channels during 10 d at room temperature, covering the velocity range −4.2 to +4.2 mm s^{-1}. Data were calibrated against an iron foil, and spectrum analysis was performed assuming Lorentzian line shapes with MossA (Prescher et al., 2012).

Conditions were far from ideal for the experiment, with (a) a small sample volume, (b) preferred orientation effects, (c) highly γ-absorbing sample constituents (Sb + Pb) and (d) broadening of nominal line widths due to deterioration (radiation damage) of the point source matrix. Despite the limitations, an asymmetric absorption doublet (asymmetry parameter $a_{12} = 0.60(2)$) is clearly identified (Fig. 4). The hyperfine parameters obtained, CS = 0.42(2) and QS = 0.89(3) mm s^{-1}, are very similar to those found for octahedrally coordinated Fe^{3+} in the synthetic isostructural compound $(Fe^{2+}_{0.5}\ Fe^{3+}_{0.5})[Sb_{1.5}Pb_{0.5}]O_4$, 0.45 and 0.85 mm s^{-1}, respectively (Berry et al., 2014). The result confirms the predominance of trivalent Fe in the igelströmite formula. Any amount of Fe^{2+}, if present, should be relatively small (< 15 % of total Fe). For manganoschafarzikite, no Mössbauer experiment was attempted because of the low Fe concentration and rarity of the crystals of this mineral.

7 Discussion and conclusions

7.1 Crystal structure and chemistry

The crystal structure of the synthetic compound Pb_3O_4 was solved by Byström and Westgren (1943). Zemann (1951a, b) described the atomic arrangements of schafarzikite and trippkeite, respectively, and showed that they are isostructural with minium. Fischer and Pertlik (1975) refined the crystal structure of schafarzikite to $R = 6$ %. The group members possess a tetragonal crystal symmetry (point group 4/*mmm*, space group $P4_2/mbc$), with unit-cell parameters $a = 8$–9 and $c \sim 6$ Å. The two- to four-valent M atoms are located on Wyckoff position 4*d* and coordinated by six O atoms in distorted (axially elongated) octahedra, which connect via trans-edges to form rutile-like ribbons along [001] (Fig. 5). The X atoms at the 8*h* position form trigonal, flattened XO_3 pyramids, which are linked via corners to form zigzag $(XO_2)_n$ chains. The X polyhedra also share corners via the terminal oxygen (O1) with two M atoms in one column and the O2 atom of an adjacent column. The non-bonding lone-pair s^2 electrons of the X ionic species (As^{3+}, Sb^{3+} or Pb^{2+}) act as pseudo-ligands and protrude into channels created by four neighbouring parallel chains (Fig. 6).

Igelströmite is isostructural with minium and the other minerals of the general formula MX_2O_4. A synthetic analogue exists, $Fe[Sb_{2-x}Pb_x]O_4$ (Whitaker et al., 2011). Their most substituted sample, $FeSb_{1.3}Pb_{0.7}O_4$, has the unit-cell parameters $a = 8.4577(1)$ and $c = 6.03652(9)$ Å (cf. Table 4). Igelströmite is derived from schafarzikite, $Fe^{2+}Sb^{3+}_2O_4$, via the coupled heterovalent substitution ${}^{M}Fe^{2+} + {}^{X}Sb^{3+} \rightarrow {}^{M}Fe^{3+} + {}^{X}Pb^{2+}$. This exchange mechanism affects only half of the Sb atoms in the unit cell. Igelströmite is thus unique in the group in that it has a mixed Sb : Pb site. The type specimen is chemically heterogeneous, with significant variations in Sb, Pb and Fe, and has a surplus of Sb^{3+} compared to the ideal formula, with 1.16–1.44 Sb atoms per formula unit (apfu) in total. This non-stoichiometry requires the presence of divalent ions to keep

Table 9. Atomic displacement factors (Å^2) for manganoschafarzikite.

Site	U^{11}	U^{22}	U^{33}	U^{23}	U^{13}	U^{12}
Sb	0.01466(11)	0.01257(10)	0.01163(11)	0	0	0.00036(6)
Mn	0.0131(2)	0.0131(2)	0.0089(3)	0	0	0.0001(2)
O1	0.0222(7)	0.0222(7)	0.0115(9)	−0.0040(6)	−0.0040(6)	0.0105(9)
O2	0.0139(10)	0.0175(10)	0.0139(9)	0	0	0.0024(8)

Table 10. Bond distances (Å) for igelströmite and manganoschafarzikite.

Igelströmite		Manganoschafarzikite	
Sb–O1 × 2	2.070(3)	Sb–O1 × 2	1.9987(11)
Sb–O2	2.051(7)	Sb–O2	1.932(2)
Mean	2.063	Mean	1.976
Fe–O1 × 2	2.097(6)	Mn–O1 × 2	2.196(2)
Fe–O2 × 4	2.064(5)	Mn–O2 × 4	2.1218(16)
Mean	2.075	Mean	2.147

the electroneutrality, achieved by some amounts of Mn^{2+} and lesser Fe^{2+}. There is also a significant As content in igelströmite, 0.17 apfu, of which a fraction needs to be assigned to the M position in the empirical formula. The bond-valence sum (Table 5) and electron density from single-crystal XRD (Table 6) data for the metal sites are anyway in reasonably good agreement with the average composition obtained from EPMA. The average ^{M}Fe–O distance in igelströmite is 2.075 Å, which is smaller than for natural (2.153 Å) and synthetic (2.159 Å) schafarzikite (Fischer and Pertlik, 1975; Whitaker et al., 2011) but quite expected as Fe^{3+} has a smaller atomic radius than Fe^{2+}, 0.645 versus 0.780 Å (Shannon, 1976).

Manganoschafarzikite is related to schafarzikite via a simple $Fe^{2+} \rightarrow Mn^{2+}$ replacement at the octahedrally coordinated sites. $MnSb_2O_4$ is a well-known synthetic compound (e.g. Chater et al., 1986; Roelsgaard et al., 2016). The average Mn–O distance in manganoschafarzikite is 2.146 Å, which is slightly smaller than the 2.153 Å of the Fe octahedron in schafarzikite (Fischer and Pertlik, 1975). For the synthetic compound, the average distance is 2.17 Å; the reduction seen in the Långban mineral is likely related to its Mg and Fe contents, 0.08 and 0.25 apfu, respectively. The average X–O distance in manganoschafarzikite, 1.976 Å, is considerably shorter than in igelströmite (2.063 Å), as anticipated from the very low content of the larger Pb^{2+} cation (0.01 apfu). The mineral is also considerably more homogeneous in terms of chemical composition than igelströmite.

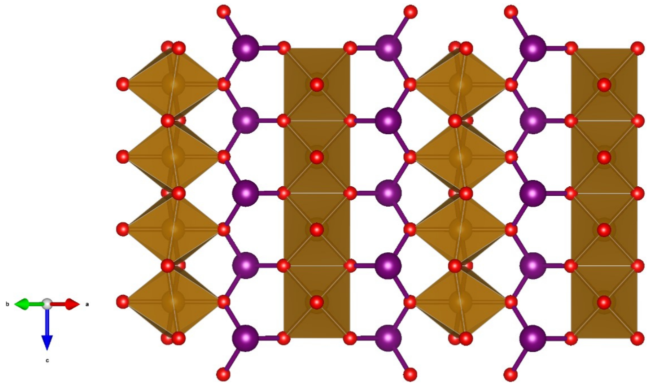

Figure 5. A (110) slice of the crystal structure of minium-group members showing the edge-sharing octahedra of M atoms (brown), interconnected via 3-coordinated X atoms (big spheres, lilac), forming trigonal XO_3 pyramids, which are linked via corners to form zigzag $(XO_2)_n$ chains. The small spheres (red, on corners of octahedra) are O atoms.

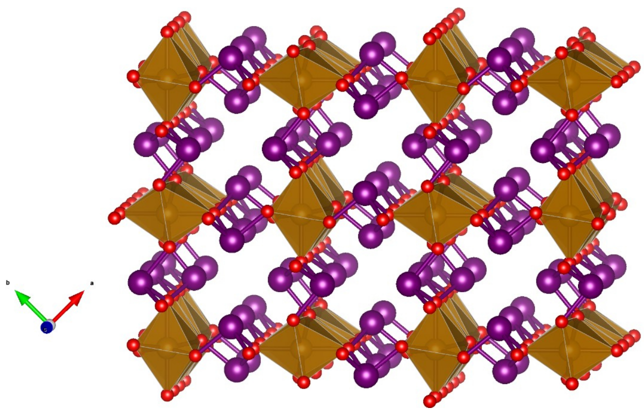

Figure 6. An oblique view along [001] showing the apical Sb(Pb) pointing into the channels between M octahedra.

7.2 Paragenesis

Igelströmite and manganoschafarzikite crystallized in open fractures, corresponding to a late paragenetic event, named "period D" by Magnusson (1930), which is connected to the most diverse stage in terms of mineral species in the evolution of the Långban deposit (Holtstam and Langhof, 1999). This episode may be related to brittle deformation and hy-

Table 11. Observed and calculated X-ray powder diffraction data (d in Å) for igelströmite and manganoschafarzikite, with the strongest peaks in bold letters.

Igelströmite					Manganoschafarzikite				
I_{meas}	d_{meas}	I_{calc}	d_{calc}	hkl	I_{meas}	d_{meas}	I_{calc}	d_{calc}	hkl
					5	6.09	3	6.117	1 1 0
14	**4.25**	8	4.2428	2 0 0	**22**	**4.30**	18	4.325	2 0 0
100	**3.21**	100	3.2140	2 1 1	**100**	**3.24**	100	3.247	2 1 1
13	3.01	12	3.0225	0 0 2	12	3.05	14	3.058	2 2 0
		7	3.0001	2 2 0	14	2.98	12	2.985	0 0 2
20	**2.69**	11	2.6993	1 1 2	**26**	**2.72**	19	2.735	3 1 0
		20	2.6833	3 1 0	11	2.68	9	2.683	1 1 2
22	**2.46**	13	2.4617	2 0 2	**20**	**2.45**	21	2.457	2 0 2
4	2.36	2	2.3642	2 1 2	6	2.36	4	2.363	2 1 2
6	2.12	4	2.1214	4 0 0	3	2.15	1	2.162	4 0 0
8	2.00	4	2.0066	3 1 2	5	2.03	5	2.039	3 3 0
		4	2.0000	3 3 0	3	2.02	3	2.017	3 1 2
19	**1.946**	18	1.9482	4 1 1	**28**	**1.976**	32	1.979	4 1 1
6	1.895	3	1.8974	4 2 0	5	1.928	4	1.934	4 2 0
14	**1.778**	16	1.7796	2 1 3	**17**	**1.767**	16	1.770	2 1 3
9	1.735	9	1.7363	4 0 2	6	1.746	6	1.751	4 0 2
16	**1.667**	17	1.6679	3 3 2	**18**	**1.680**	20	1.683	3 3 2
9	1.524	9	1.5247	5 2 1	6	1.548	6	1.551	5 2 1
4	1.511	4	1.5112	0 0 4	5	1.492	4	1.492	0 0 4
3	1.4556	2	1.4578	5 1 2	6	1.473	5	1.483	5 3 0
		2	1.4552	5 3 0			5	1.475	5 1 2
5	1.4383	6	1.4398	4 1 3	**15**	**1.441**	10	1.444	4 1 3
4	1.4121	4	1.4142	6 0 0			5	1.441	6 0 0
					1	1.340	2	1.341	2 2 4
					4	1.326	3	1.328	5 3 2
					8	1.315	5	1.317	5 4 1
3	1.3152	4	1.3167	3 1 4	7	1.310	3	1.310	3 1 4
4	1.2933	4	1.2944	5 4 1					
2	1.2800	1	1.2809	6 0 2					
2	1.2417	4	1.2412	5 2 3					

Calculated data were obtained through VESTA 3 (Momma and Izumi, 2011).

drothermal mobilization and precipitation of previously enriched elements, occurring during the ~ 1 Ga Sveconorwegian orogeny that mildly affected this part of the Bergslagen region (Bingen et al., 2021). The different fracture systems normally crosscut the local ore bodies at Långban, and the specific kind of substrate lithology (Fe ore, Mn ore, skarn, etc.) might have an influence on late-stage mineral formation.

Compounds of the present type can be produced at a wide range of temperatures as seen from synthesis experiments, hydrothermally at about 200 °C (Đorđević et al., 2015) and by solid-state reactions up to 1200 °C (Whitaker et al., 2011). Micro-thermometric data from fluid inclusions of minerals in late-fissure Pb–As–Sb–Mn assemblages at the deposit indicate formation temperatures below 180 °C and a close to near-surface, low-pressure regime (Jonsson and Broman, 2002). The conditions of formation here were reduced enough to stabilize Sb^{3+} and Fe^{2+} in the present new minerals but probably less so than in the more persistent native lead–pyrochroite veins characteristic of the Långban D period (Boström, 2002) and in other late-formed mineral assemblages containing native elements (As, Sb). It is notable that in earlier-formed skarn matrices, Sb has only been observed in the pentavalent form in the Långban-type deposits (Holtstam et al., 1998). Crystallization of igelströmite and manganoschafarzikite is probably possible within a wide range of pH conditions (see Leverett et al., 2012). Although minor quantities of late-stage sulfides are present in some fissures in the deposit, the formation of Sb–S species like stibnite, gudmundite or berthierite in the present system has been prevented by higher-pH and higher-fO_2 conditions than what are favourable for sulfide precipitation (Williams-Jones and Norman, 1997). A hydrothermal (rather than supergene) origin of schafarzikite was also inferred from the type locality, the Krížnica (Pernek) Sb deposit in the Slovak Republic (Sejkora et al., 2007).

7.3 Nomenclature of the minium mineral group

The group encompasses tetragonal minerals of the general formula MX_2O_4 (X denotes ion with a lone electron pair, e.g. As^{3+}, Sb^{3+}, or Pb^{2+}) and currently includes five valid members: in chronological order, minium, trippkeite, schafarzikite, igelströmite and manganoschafarzikite (Table 1). Apuanite, $(Fe^{2+}Fe^{3+}_2)(Fe^{3+}_2Sb^{3+}_4)O_{12}S$, and versiliaite, $(Fe^{2+}_2Fe^{3+}_2)(Fe^{3+}_2Sb^{3+}_6)O_{16}S$, are direct structural derivatives (Mellini and Merlino, 1979) but not counted in the minium group because of mixed anion compositions (following the introduction of extra S^{2-} to charge-balance Fe^{3+} in the octahedral ribbons). Kusachiite, $CuBi_2O_4$ (Henmi, 1995), which used to belong to the previous informal trippkeite group (Back, 2022), crystallizes in space group $P4/ncc$. The Cu^{2+} ion in kusachiite is located at the Wyckoff position 4c, and has 4-fold (square planar rather than octahedral) coordination to O, whereas Bi occurs in BiO_4 polyhedra (Boivin et al., 1976). Leiteite, $ZnAs_2O_4$, also has a different and unique crystal structure in relation to the minium group, but Ghose et al. (1987) hypothesized a polymorph isostructural to the group to exist at high pressures. Dinnebier et al. (2003) showed that minium undergoes a displacive phase transition > 6 GPa to another structure type with space group $Pbam$.

The group members belong to a family of compounds studied by material scientists because of potential functional properties, e.g. as ferroelectrics (Bennet and Rabe, 2012). The plethora of synthetic equivalents suggests that more minerals could exist. There is no intention here to impose a strict nomenclature scheme to dictate the names of future members, but we recommend adhering to the existing minerals for root names, based on the X atom content, and add prefixes for elements substituting at M sites. For example, isostructural $CoAs_2O_4$ would then be "cobaltotrippkeite", $MgSb_2O_4$ "magnesioschafarzikite" and $SnPb_2O_4$ "stannominium". The minerals of the group, except minium itself, fits in the Nickel–Strunz group 4.JA (arsenites, antimonites, bismuthites; without additional anions, without H_2O).

Data availability. CIF files are deposited in the Supplement.

Supplement. The supplement related to this article is available online at: https://doi.org/10.5194/ejm-36-311-2024-supplement.

Author contributions. JL observed the unknown minerals and obtained physical descriptions. DH and AK collected and interpreted spectroscopic data. HF carried out the single-crystal X-ray diffraction experiments and executed structural refinements. ME performed the microprobe analyses. DH and JL wrote the text, in consultation with all authors.

Competing interests. The contact author has declared that none of the authors has any competing interests.

Acknowledgements. Torbjörn Lorin is thanked for the colour photographs.

Financial support. Publication costs were covered by the Finneman fund (Royal Swedish Academy of Sciences).

Review statement. This paper was edited by Cristiano Ferraris and reviewed by Daniel Atencio and one anonymous referee.

References

Agricola, G.: "De Re Metallica", The Mining Magazine, London, Salisbury house, 640 pp., 1912 (Translated by H. C. Hoover and L. H. Hoover).

Back, M. E.: "Fleischer's glossary of mineral species", Mineralogical Association of Canada, ISBN 978-0-921294-64-1, 2022.

Bennett, J. W. and Rabe, K. M.: Integration of first-principles methods and crystallographic database searches for new ferroelectrics: Strategies and explorations, J. Solid State Chem., 195, 21–31, https://doi.org/10.1016/j.jssc.2012.05.013, 2012.

Berry, F. J., de Laune, B. P., Greaves, C., Whitaker, M. J., Thomas, M. F., and Marco, J. F.: Mössbauer spectroscopy in the investigation of new mineral–related materials, Hyperfine Interact., 226, 545–552, https://doi.org/10.1007/s10751-013-0967-6, 2014.

Bingen, B., Viola, G., Möller, C., Vander Auwera, J., Laurent, A., and Yi, K.: The Sveconorwegian orogeny, Gondwana Res., 90, 273–313, https://doi.org/10.1016/j.gr.2020.10.014, 2021.

Boivin, J. C., Tréhoux, J., and Thomas, D.: Étude structurale de $CuBi_2O_4$, B. Minéral. 99, 193–196, https://doi.org/10.3406/bulmi.1976.7065, 1976.

Boström, K., Rydell, H., and Joensuu, O.: Långban – An exhalative sedimentary deposit?, Econ. Geol., 74, 1002–1011, https://doi.org/10.2113/gsecongeo.74.5.1002, 1979.

Boström, K.: Late hydrothermal events at Långban–how many and how alkaline?, GFF, 124, 236–237, https://doi.org/10.1080/11035890201244236, 2002.

Byström, A. and Westgren, A.: The crystal structure of Pb_3O_4 and $SnPb_2O_4$, Arkiv Kem. Mineral. Geol. B, 16, 1–7, 1943.

Chater, R., Gavarri, J. R., and Genet, F.: Composes isomorphes $MeX_2O_4E_2$: I. Etude vibrationnelle de $MnSb_2O_4$ entre 4 et 300 K: champ de force et tenseur élastique, J. Solid State Chem., 63, 295–307, https://doi.org/10.1016/0022-4596(86)90181-7, 1986.

Damour, A. and vom Rath, G.: Ueber den Trippkeït, eine neue Mineralspecies, Z. Kristallogr., 5, 245–249, 1880.

Dinnebier, R. E., Carlson, S., Hanfland, M., and Jansen, M.: Bulk moduli and high-pressure crystal structures of minium, Pb_3O_4, determined by X-ray powder diffraction, Am. Mineral., 88, 996–1002, https://doi.org/10.2138/am-2003-0707, 2003.

Đorđević, T., Wittwer, A., Jagličić, Z., and Djerdj, I.: Hydrothermal synthesis of single crystal $CoAs_2O_4$ and $NiAs_2O_4$ compounds and their magnetic properties, RSC Adv., 5, 24, 18280–18287, https://doi.org/10.1039/C4RA16122J, 2015.

Farrugia, L. J.: WinGX and ORTEP for Windows: and update, J. Appl. Crystallogr., 45, 849–854, https://doi.org/10.1107/S0021889812029111, 2014.

Fischer, R. and Pertlik, F.: Verfeinerung der Kristallstruktur des Schafarzikits, $FeSb_2O_4$, Tscher. Miner. Petrog., 22, 236–241, https://doi.org/10.1007/BF01087842, 1975.

Flink, G.: Lista på mineral från Långban, som kräva undersökning, Geol. Fören. Stock. För., 43, 195–201, 1921.

Flink, G.: XVIII. Über die Långbansgruben als Mineralvorkommen, Eine vorläufige Orientierung, Z. Kristallogr., 58, 356–385, 1923.

Gagné, O. C. and Hawthorne, F. C.: Comprehensive derivation of bond-valence parameters for ion pairs involving oxygen, Acta Crystallogr. B, 71, 562–578, https://doi.org/10.1107/S2052520615016297, 2015.

Gavarri, J. R. and Weigel, D.: Oxydes de plomb, I. Structure cristalline du minium Pb_3O_4, à température ambiante (293 K), J. Solid. State Chem., 13, 252–257, https://doi.org/10.1016/0022-4596(75)90127-9, 1975.

Gettens, R. J., Feller, R. L., and Chase, W. T.: Vermilion and cinnabar, Stud. Conserv., 17, 45–69, https://doi.org/10.1179/sic.1972.006, 1972.

Ghose, S., Sen Gupta, P. K., and Schlemper, E. O.: Leiteite, $ZnAs_2O_4$; a novel type of tetrahedral layer structure with arsenite chains, Am. Mineral., 72, 629–632, 1987.

Heddle, M.: The geognosy and mineralogy of Scotland, Islands of Uya, Haaf Grunay, Fetlar, and Yell, Mineral. Mag., 2, 106–133, 1878.

Henmi, C.: Kusachiite, $CuBi_2O_4$, a new mineral from Fuka, Okayama Prefecture, Japan, Mineral. Mag. 59, 545–548, https://doi.org/10.1180/minmag.1995.059.396.14, 1995.

Holland, T. J. B. and Redfern, S. A. T.: Unit cell refinement from powder diffraction data: the use of regression diagnostics, Mineral. Mag., 61, 65–77, https://doi.org/10.1180/minmag.1997.061.404.07, 1997.

Holtstam, D. and Langhof, J. (Eds): Långban: the mines, their minerals, geology and explorers, Naturhistoriska riksmuseet and Raster Förlag, Stockholm, ISBN 91 87214 881, 1999.

Holtstam, D. and Mansfeld, J.: Origin of a carbonate-hosted Fe-Mn-(Ba-As-Pb-Sb-W) deposit of Långban-type in Central Sweden, Mineral. Dep., 36, 641–657, https://doi.org/10.1007/s001260100183, 2001.

Holtstam, D., Nysten, P., and Gatedal, K.: Parageneses and compositional variations of Sb oxyminerals from Långban-type deposits in Värmland, Sweden, Mineral. Mag., 62, 395–407, https://doi.org/10.1180/002646198547666, 1998.

Igelström, L. J.: Nya och sällsynta mineralier från Vermlands och Örebro län, Öfversigt Kongl. Vetenskap. Akad. För., 22, 605–611, 1865.

Jonsson, E. and Broman, C.: Fluid inclusions in late-stage Pb-Mn-As-Sb mineral assemblages in the Långban deposit, Bergslagen, Sweden, Can. Mineral., 40, 47–65, https://doi.org/10.2113/gscanmin.40.1.47, 2002.

Kharbish, S.: Raman spectra of minerals containing interconnected $As(Sb)O_3$ pyramids: trippkeite and schafarzikite, J. Geosci., 57, 53–62, https://doi.org/10.3190/jgeosci.111, 2012.

Krenner, J. A.: Schafarzikit, ein neues mineral, Z. Kristallogr., 56, 198–200, 1921.

Langhof, J.: “Mineralogists and collectors”, in: Holtstam and Langhof: “Långban – The mines, their minerals, geology and explorers”, Raster förlag and Swedish Museum of Natural History, Stockholm, ISBN 91 87214 881, 1999.

Leverett, P., Reynolds, J. K., Roper, A. J., and Williams, P. A.: Tripuhyite and schafarzikite: two of the ultimate sinks for antimony in the natural environment, Mineral. Mag., 76, 891–902, https://doi.org/10.1180/minmag.2012.076.4.06, 2012.

Magnusson, N. H.: Långbans malmtrakt, Sver. Geol. Undersök, Ca, 23, 1–111, 1930.

Mellini, M. and Merlino, S.: Versiliaite and apuanite: Derivative structures related to schafarzikite, Am. Mineral., 64, 1235–1242, 1979.

Momma, K. and Izumi, F.: VESTA 3 for three-dimensional visualization of crystals, volumetric and morphology data, J. Appl. Crystallogr., 44, 1272–1276, https://doi.org/10.1107/S0021889811038970, 2011.

Prescher, C., McCammon, C., and Dubrovinsky, L.: MossA: a program for analyzing energy-domain Mössbauer spectra from conventional and synchrotron sources, J. Appl. Cryst., 45, 329–331, https://doi.org/10.1107/S0021889812004979, 2012.

Rackham, H.: “Pliny: Natural History”, Volume IX, Books 33–35, Loeb Classical Library No. 394, Harvard University Press, 111–124, 1952.

Roelsgaard, M., Nørby, P., Eikeland, E., Søndergaard, M., and Iversen, B. B.: The hydrothermal synthesis, crystal structure and electrochemical properties of $MnSb_2O_4$, Dalton Transact., 45, 18994–19001, https://doi.org/10.1039/C6DT03459D, 2016.

Sejkora, J., Ozdín, D., Vitálos, Tucek, P., Cejka, J., and Duda, R.: Schafarzikite from the type locality Pernek (Malé Karpaty Mountains, Slovak Republic) revisited, Eur. J. Mineral., 19, 419–427, https://doi.org/10.1127/0935-1221/2007/0019-1723, 2007.

Shannon, R. D.: Revised effective ionic radii and systematic studies of interatomic distances in halides and chalcogenides, Acta Crystallogr. A, 32, 751–767, https://doi.org/10.1107/S0567739476001551, 1976.

Sheldrick, G. M.: Crystal structure refinement with SHELXL, Acta Crystallogr. C, 71, 3–8, https://doi.org/10.1107/S2053229614024218, 2015.

Smithson, J.: Account of a discovery of native minium, in: a letter from James Smithson, FRS to the Right Hon. Sir Joseph Banks, Philos. T. R. Soc. Lond., 96, 267–268, 1806.

Weibull, M.: Några manganmineral från Vester-Silfberget i Dalarne, Geol. Fören. Stock. För., 6, 499–509, 1883.

Whitaker, M. J., Bayliss, R. D., Berry, F. J., and Greaves, C.: The synthesis, structure, magnetic and electrical properties of $FeSb_{2-x}Pb_xO_4$, J. Mater. Chem., 21, 14523–14529, https://doi.org/10.1039/C1JM12645H, 2011.

Williams-Jones, A. E. and Norman, C.: Controls of mineral parageneses in the system Fe-Sb-S-O, Econ. Geol., 92, 308–324, https://doi.org/10.2113/gsecongeo.92.3.308, 1997.

Zemann, J.: Formel und Kristallstruktur des Schafarzikits, Tscher. Miner. Petrog., 2, 166–175, https://doi.org/10.1007/BF01127892, 1951a.

Zemann, J.: Formel und Kristallstruktur des Trippkeits, Tscher. Miner. Petrog., 2, 417–423, https://doi.org/10.1007/BF01135291, 1951b.